

# Eph/ephrins and N-cadherin coordinate to control the pattern of sympathetic ganglia

Jennifer C. Kasemeier-Kulesa<sup>1,2</sup>, Roger Bradley<sup>2</sup>, Elena B. Pasquale<sup>3</sup>, Frances Lefcort<sup>2</sup> and Paul M. Kulesa<sup>1,\*</sup>

Previous studies have suggested that the segmental pattern of neural-crest-derived sympathetic ganglia arises as a direct result of signals that restrict neural crest cell migratory streams through rostral somite halves. We recently showed that the spatiotemporal pattern of chick sympathetic ganglia formation is a two-phase process. Neural crest cells migrate laterally to the dorsal aorta, then surprisingly spread out in the longitudinal direction, before sorting into discrete ganglia. Here, we investigate the function of two families of molecules that are thought to regulate cell sorting and aggregation. By blocking Eph/ephrins or N-cadherin function, we measure changes in neural crest cell migratory behaviors that lead to alterations in sympathetic ganglia formation using a recently developed sagittal slice explant culture and 3D confocal time-lapse imaging. Our results demonstrate that local inhibitory interactions within inter-ganglionic regions, mediated by Eph/ephrins, and adhesive cell-cell contacts at ganglia sites, mediated by N-cadherin, coordinate to sculpt discrete sympathetic ganglia.

**KEY WORDS:** Ephrin, N-cadherin, Neural crest, Sympathetic ganglia, Chick, Confocal, Time-lapse imaging

## INTRODUCTION

Neural crest cells are a migratory population of pluripotent cells (LeDouarin and Kalcheim, 1999) that emerge from the dorsal neural tube along the vertebrate axis (Garcia-Castro et al., 2000; Bronner-Fraser, 1986) and migrate along stereotypical pathways through the embryo (Newgreen et al., 1986; Loring and Erickson, 1987; Schilling and Kimmel, 1994; Kulesa and Fraser, 2000; Trainor and Krumlauf, 2002) to populate specific peripheral targets (Kontges and Lumsden, 1996; Bronner-Fraser, 1986). Based on their axial level of origin, neural crest cells give rise to vastly diverse derivatives. Specifically, trunk neural crest cells give rise to components of the enteric nervous system, melanocytes, dorsal root and sympathetic ganglia (LeDouarin and Kalcheim, 1999). Sympathetic ganglia are crucial for proper function of the autonomic peripheral nervous system, including blood pressure regulation, vasal dilation and smooth muscle control. Trunk neural crest cells migrate through the rostral portion of each somite, forming a repeating pattern of discrete cell migratory streams (Rickmann et al., 1985; Bronner-Fraser, 1986; Tosney and Oakley, 1990; Krull et al., 1995). Molecular analyses have confirmed that complementary expression of ephrinB1 (on the caudal half of somites) and its receptor EphB2 (on trunk neural crest cells) mediate neural crest cell-substrate interactions that sculpt chick trunk neural crest cells into discrete migratory streams (Wang and Anderson, 1997; Krull et al., 1997). As each discrete trunk neural crest cell migratory stream terminates ventral to a rostral half-somite, there has been speculation that sympathetic ganglion formation is the direct result of the iterated neural crest cell migratory stream pattern imposed by the somite (Bronner-Fraser, 1986; Lallier and Bronner-Fraser, 1988; Oakley and Tosney, 1993).

The cellular and molecular mechanisms that drive neural crest cells to segregate into discrete ganglia have not yet been elucidated due to the lack of a model system to assay and monitor the affects of potential molecules and signals influencing neural crest cell behavior. Recently, using intravital time-lapse confocal microscopy, we described in detail the spatiotemporal migration of chick neural crest cells through the somites and their arrival at sympathetic ganglion target sites (Kasemeier-Kulesa et al., 2005). Surprisingly, upon arrival at the sympathetic ganglion target sites, neural crest cells deviate dramatically from their segregated pattern and spread out in the anterior and posterior directions. The neural crest cells then undergo a later re-sorting into discrete ganglia (Kasemeier-Kulesa et al., 2005). In this study, we investigated the molecular mechanisms that mediate the segregation of neural crest cells into discrete sympathetic ganglia. We mechanistically tested two hypotheses for the formation of discrete sympathetic ganglia: (1) the sorting of trunk neural crest cells into discrete sympathetic ganglia results from an Eph-ephrin repulsion in the inter-ganglionic regions (the regions ventral to the caudal somite, between presumptive sympathetic ganglia); and/or (2) that a local cell-adhesion-mediated interaction drives the aggregation and coalescence of neural crest cells into discrete sympathetic ganglia. Using *in vivo* 3D confocal time-lapse imaging coupled with molecular perturbations, we demonstrate that, in fact, both mechanisms are operative: N-cadherin mediates attractive interactions and Eph/ephrin mediates repulsive interactions to sculpt neural crest cells into discrete sympathetic ganglia.

## MATERIALS AND METHODS

### Embryos

Fertilized White Leghorn chicken eggs (Ozark Hatchery, Meosho, MO) were placed in an incubator at 38°C (Kuhl, Flemington, NJ). Eggs were rinsed with 70% alcohol and 3 ml albumin removed. Eggs were windowed and embryos staged according to Hamburger and Hamilton (HH) (Hamburger and Hamilton, 1951). Embryos at HH St. 10 were injected with an EGFP-encoding plasmid, pMES, 4.3 µg/ml, to fluorescently label premigratory neural crest cells located in the dorsal neural tube. pMES is a control EGFP empty vector that utilizes the chick β-actin promoter and internal IRES site. Fast Green FCF (Sigma, F-7252; 10 µg/ml) was added 1:5 to the injection needle to visualize injection of the construct. The EGFP-

<sup>1</sup>Stowers Institute for Medical Research, 1000 E. 50th St., Kansas City, MO 64110, USA. <sup>2</sup>Cell Biology and Neuroscience Department, Montana State University, Bozeman, MT 59717, USA. <sup>3</sup>Developmental Neurobiology Department, The Burnham Institute, La Jolla, CA 92037, USA.

\*Author for correspondence (e-mail: pmk@stowers-institute.org)

plasmid was microinjected into the lumen of the neural tube using a borosilicate glass capillary pulled needle (World Precision Instruments, MTW100-4) until the region of the neural tube between the forelimbs and hind limbs was filled. Constructs were electroporated into premigratory neural crest cells using gold-coated Genetrode electrodes (Fisher, BTX512) and electroporator (Genetronics, San Diego, CA) with five 50-millisecond pulses of 20 volts. Eggs were resealed with adhesive tape and incubated at 38°C for 2-3 days, then selected for brightness and uniformity of EGFP labeling.

#### Antibody-function-blocking injections

Embryos electroporated with EGFP at HH St. 10 (previously described) were used for these experiments. EGFP-labeled embryos at E3 were surveyed using a fluorescence dissecting microscope (Carl Zeiss, Stemi SV11). EphB2-Fc (100 µg/ml), ephrinB1-Fc (100 µg/ml), and Fc-control (100 µg/ml) fusion proteins were obtained from R&D Laboratories (467-B2-200, 473-EB-200, 110-HG, respectively). Fast Green FCF (Sigma, F-7252) was added to fusion proteins at 1:10 to visualize injection of fusion protein blocking reagents in ovo. By HH St. 17, neural crest cells have migrated through the somite and reached the dorsal aorta (Fig. 1A-C). Using HH St. 17 embryos, we microinjected either EphB2-Fc, ephrinB1-Fc or Fc-control immediately lateral to neural crest cells dispersed along the anteroposterior axis adjacent to the dorsal aorta, injecting a bolus of inhibitor the length of one-half to one somite (Fig. 2). Briefly, a hole was made in the vitelline membrane above the ventral edge of the somites. The needle filled with Fc-fusion proteins was attached to a micromanipulator (World Precision Instruments, M3301) for fine control of placement and injection within the embryo. The tip of the needle was brought down adjacent to the ventral edge of the somites and the corridor where neural crest cells were dispersed. A picospritzer (Picospritzer III; Parker Hannifin Corporation) was used to deliver a small bolus of Fc-fusion proteins. Eggs were resealed with adhesive tape and incubated at 38°C for 24-36 hours. After this incubation period, live embryos were removed from the egg (Krull and Kulesa, 1998), fixed in 4% paraformaldehyde (PFA), mounted on 22×75 mm microslides (VWR 48314-024), and imaged using an inverted laser scanning confocal

microscope (Zeiss Pascal LSM). As an internal control, effects of inhibitory Fc-fusion bodies were analyzed anterior and posterior to the site of inhibitor injection. NCD2 blocking antibody (300 µg/ml), and Hu rat IgG (control for NCD2; from P. Henion and J. Weston, University of Oregon) were injected and analyzed in the same location and manner as Eph/ephrin Fc-fusion proteins.

#### Electroporation of misexpressing cadherin vectors

Wild-type chicken N-cadherin (gift of M. Takeichi) and dominant negative cadherin, CBR (Riehl et al., 1996), were subcloned into the pMES expression vector. Fast Green FCF was added to CBR-pMES (dominant negative cadherin; 4.0 µg/ml) and NCad-pMES (full-length N-cadherin) 1:10. Plasmids were electroporated in ovo into HH St. 10 embryos (see above) to label premigratory neural crest cells and reincubated. Embryos were harvested at E3-E4, fixed in 4% PFA and sympathetic ganglia were analyzed.

#### Embryo preparation for sagittal cultures

HH St. 10 embryos were injected with EGFP control or misexpressing constructs (described above). Embryos were reincubated for 2-3 days when further manipulation was performed (i.e. inhibitor injection). Embryos were harvested in Ringer's solution, membranes removed and sagittal explants made (Kasemeier et al., 2004). Sagittal explants were transferred to Millipore culture plate inserts (Millipore, PICMORG50) coated with 20 µg/ml fibronectin (Gibco, 33016-015) cut side down. Culture insert and sagittal explant were then transferred to a glass bottom 35 mm Petri dish (MatTek Corp., P35G-0-14-C). Neurobasal medium (Gibco, 21103-049), supplemented with 20 mM B27 (Gibco, 17504-044) was added to the bottom of the glass bottom Petri dish. The Petri dish was sealed with parafilm and imaged on a Zeiss Pascal LSM.

#### Static and 3D confocal time-lapse microscopy

Fixed, EGFP-labeled explants were visualized using a Zeiss Pascal LSM. For time-lapse microscopy, the microscope was surrounded with a snug-fitting cardboard box and thermal insulation (Reflectix, BP24025) with a

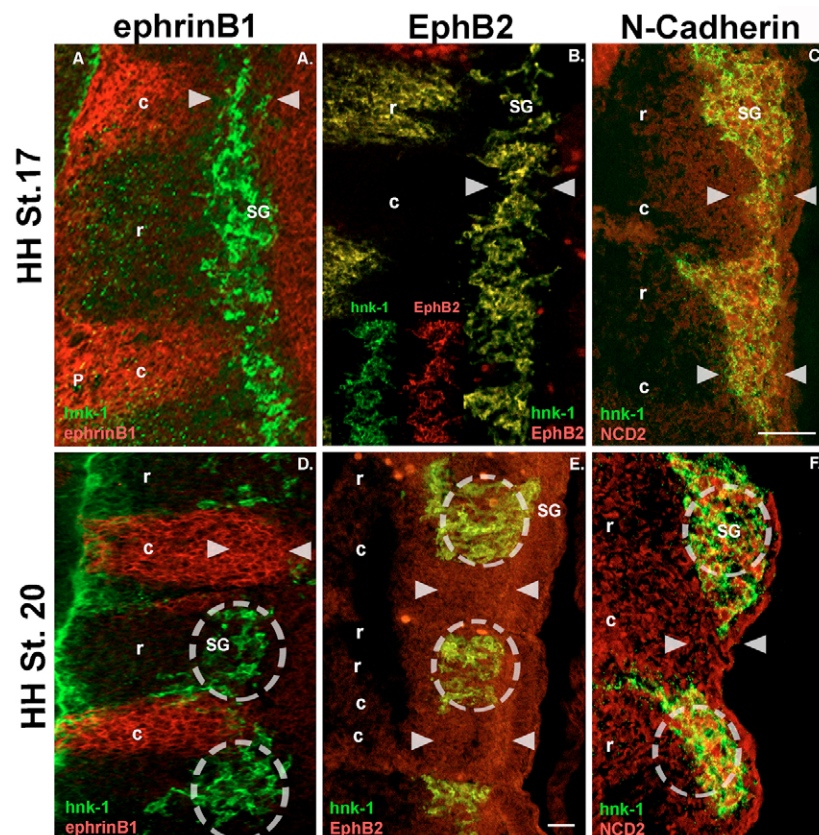


**Fig. 1. Expression patterns of ephrinB1, EphB2 and N-cadherin.** Changes in Eph/ephrin and N-cadherin expression correlate in space and time with neural crest cell segregation from inter-ganglionic regions and sorting into sympathetic ganglia. Immunohistochemistry performed on HH St. 17 and HH St. 20 sagittal cryostat sections, 15 µm. (A-C) HH St. 17 sections. hnk-1-labeled (green) neural crest cells dispersed adjacent to the dorsal aorta. (D-F) HH St. 20 sections. hnk-1-labeled (green) neural crest cells formed sympathetic ganglia adjacent to the rostral somite. (A) ephrinB1 (red) expressed in caudal somite. Expression ends at ventral edge of caudal somite, arrowheads. (D) ephrinB1 (red) expressed in inter-ganglionic regions between sympathetic ganglia anlagen, arrowheads. (B) EphB2 (red) coexpressed on hnk-1-labeled neural crest cells in the rostral somite and dispersed adjacent to the dorsal aorta. Inset shows separate green channel (hnk-1) and red channel (EphB2). (E) EphB2 (red) coexpressed on neural crest cells that formed sympathetic ganglia. (C) NCD2 (red) expressed on neural crest cells dispersed adjacent to dorsal aorta. (F) NCD2 (red) expressed in sympathetic ganglia. Arrowheads indicate inter-ganglionic region, dashed circles indicate sympathetic ganglia. Scale bars: in C, 20 µm for A-C,F; in E, 20 µm for D,E, c, caudal somite; r, rostral somite; SG, sympathetic ganglia.

tabletop incubator (Lyon Electric, 950-107) fed into one side of the box (Krull and Kulesa, 1998). The fluorescent EGFP plasmid was excited with the 488 nm laser line and FITC filter and all other imaging parameters were as described in Kasemeier et al. (Kasemeier et al., 2004).

### Immunohistochemistry

Embryos were collected in PBS and fixed in 4% PFA for 4 hours. Embryos for cryostat sectioning were rinsed in PBS, run up in a sucrose gradient (5%, 15%, 30% in PBS), embedded in OCT and stored at  $-80^{\circ}\text{C}$ . Sagittal cryostat sections were obtained at 15  $\mu\text{m}$  thickness. Embryos for whole-mount staining were fixed as above, washed in PBS, blocked as previously described (Rifkin et al., 2000) and incubated in primary antibodies for 2-3 days at  $4^{\circ}\text{C}$ . Primary antibodies included: Hnk-1 (Developmental Studies Hybridoma Bank, University of Iowa), NCD2 (kind gift of M. Takeichi, Riken Center, Japan), EphB2 [anti-Cek5 (897-995) (Holash et al., 1995)] and ephrinB1 (Koblar et al., 2000). Embryos were then washed and blocked at room temperature for 1 hour before incubation in secondary antibody overnight at  $4^{\circ}\text{C}$ . Embryos were then washed with PBS and stored in  $1\times$  PBS at  $4^{\circ}\text{C}$ .

Slides with sectioned embryos for immunohistochemistry were removed from  $-80^{\circ}\text{C}$  and rehydrated in Tris-buffered saline (TBS) for 20 minutes. Slides were washed with TBS + 0.5% Triton X-100 and blocked with TBS + 0.5% Triton X-100 + 20% goat serum and 0.01 mol/l glucose for 1 hour at room temperature. Primary antibody applied in blocking solution at  $4^{\circ}\text{C}$  overnight. Slides were washed and incubated for 1 hour in block at room temperature. Secondary antibody applied for 1 hour in block at room temperature. Slides were washed and coverslipped using the ProLong Antifade reagent kit (Molecular Probes, P-7481).

### Data analysis

Images were collected, processed and analyzed using Zeiss AIM software. Measurement calculations were performed using AIM software. AIM software stores objective information and calculates distances in micrometers from pixel width. Filopodia counts (only over 1  $\mu\text{m}$  in thickness), cell speeds, displacement and meandering rates were calculated using Volocity software (Improvision). Statistical analysis was performed using Student's *t*-test.

## RESULTS

### The spatiotemporal expression of ephrinB1 and EphB2 correlates with sorting of neural crest cells into discrete sympathetic ganglia

Our first goal was to identify candidate molecules with a spatiotemporal expression pattern that correlated with the movements of neural crest cells from inter-ganglionic regions. As ephrinB1 and its receptor, EphB2, have been shown to be expressed in complementary patterns and restrict neural crest cell migration to the rostral somite, we tested whether EphB2/ephrinB1 expression near the dorsal aorta correlated with changes in neural crest cell migratory behaviors. Using immunohistochemistry and antibodies to ephrinB1, EphB2 and Hnk-1 to identify neural crest cells, we examined expression patterns in the chick trunk during sympathetic ganglia formation (Fig. 1A,B,D,E; E2.5-3.5; HH St. 17-21). At HH St. 17, neural crest cells were dispersed along a corridor between the ventral edge of the somite and dorsal aorta in a continuous stream (Fig. 1A,B). By HH St. 20, neural crest cells have re-sorted to form discrete sympathetic ganglia (Fig. 1D,E) (Kasemeier-Kulesa et al., 2005). Interestingly, at HH St. 17, ephrinB1 was absent from this corridor where neural crest cells dispersed (Fig. 1A, arrowheads). EphrinB1 was localized to the caudal somite as expected, but only extended to the ventral edge of the somite (Fig. 1A). By contrast, EphB2 at HH St. 17 is expressed in neural crest cells that are spread along the corridor between the ventral somite and dorsal aorta and by Hnk-1 positive neural crest cells in the rostral somite (Fig. 1B) (Santiago and Erickson, 2002; Krull et al., 1997).

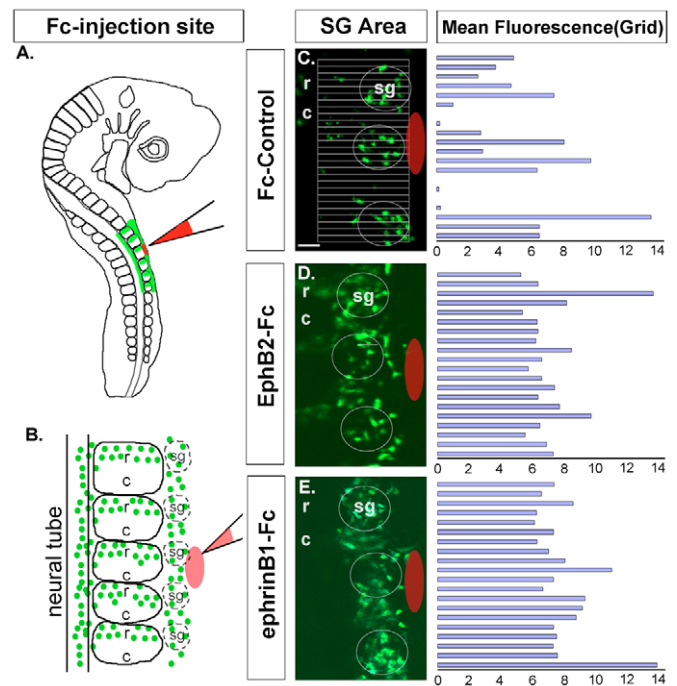


**Fig. 2. EphB2 and ephrinB1 fusion proteins disrupt proper sympathetic ganglia formation.** (A) E3 embryo schematic with EGFP-labeled trunk neural crest cells migrating through the rostral somite and dispersed adjacent to the dorsal aorta. The red oval indicates axial level and size of the fusion protein injection. (B) Magnified trunk region of the embryo where the inhibitor was injected, showing focal delivery the length of one somite (red oval). (C) IgG-Fc-control injected embryo ( $n=8$ ) with normal sympathetic ganglia formed adjacent to the rostral somite. The horizontal grid indicates the rows where mean fluorescence intensity was calculated, and plotted onto the graph to the right. (D) EphB2-Fc injected embryos ( $n=6$ ). Neural crest cells found along the anteroposterior axis of the dorsal aorta in a random orientation. Circles indicate the location of presumptive sympathetic ganglia. (E) ephrinB1-Fc injected embryo ( $n=6$ ). Neural crest cells evenly distributed along the anteroposterior axis of the dorsal aorta. The red oval indicates the inhibitor injection site. Scale bar: 20  $\mu\text{m}$ . c, caudal somite; r, rostral somite; sg, sympathetic ganglion.

Between HH St. 17 and 20, the spatial extent of ephrinB1 expression increases from the ventral edge of the somite into mesodermal tissue in the presumptive inter-ganglionic regions. By HH St. 20, ephrinB1 is expressed from the ventral edge of the somites into the mesodermal tissue in the presumptive inter-ganglionic regions (Fig. 1D, arrowheads). Interestingly, neural crest cells that were dispersed between presumptive sympathetic ganglia sites at HH St. 17 emigrate away from the inter-ganglionic region and condense to form discrete ganglia by HH St. 20 (Fig. 1D-F; circled regions). Neural crest cells condense to form discrete ganglia ventral to the rostral half of each somite, and our data show that EphB2 expression is maintained on neural crest cells as they condense to form sympathetic ganglia (Fig. 1E). EphrinB1 was still expressed in the caudal portion of each somite and remaining neural crest cells in the rostral somite expressed EphB2 (data not shown). Thus, there is a temporal correlation between the extension of ephrinB1 expression into mesodermal tissue in the inter-ganglionic regions and the directed movement of neural crest cells away from these regions into discrete ganglia.

### Blocking EphB2 or ephrinB1 inhibits segregation of sympathetic ganglia

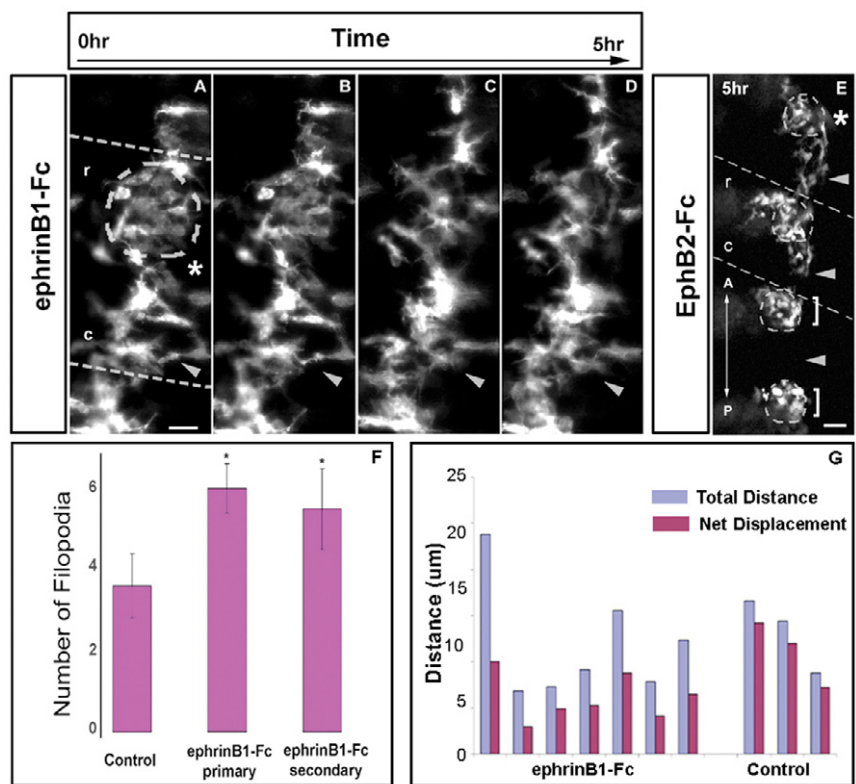
Given the spatiotemporal correlation between these gene expression patterns and neural crest cell movements in the inter-ganglionic regions, we tested the hypothesis that ephrinB1 and EphB2 play a role in neural crest cell sorting. To block signaling in ovo, we utilized ephrinB1 and EphB2 fusion proteins. These Fc-fusion proteins compete for binding to their endogenous respective proteins and abrogate signaling that would normally be stimulated by EphB2-expressing neural crest cells binding ephrinB1 (Krull et al., 1997). Embryos were injected and electroporated in ovo with the EGFP-plasmid pMES into the neural tube of HH St. 10 embryos to label premigratory neural crest cells. By HH St. 17, neural crest cells have arrived ventrally to the rostral somite and are dispersed along an anteroposterior corridor adjacent to the dorsal aorta. We focally injected Fc-fusion proteins in ovo immediately lateral to neural crest cells along the dorsal aorta at HH. St. 17, before the sympathetic ganglia sorting process (Fig. 2A,B, red ovals). We injected at this time point, as injecting Fc-fusion proteins, dominant negative or siRNA constructs earlier would affect premigratory neural crest cells and their initial migration through the somites. Thus our experimental strategy was designed to avoid any perturbation of neural crest cell migration before the cells had arrived at the dorsal aorta. After 24 hours of reincubation (>HH St. 20), when neural crest cells should have formed discrete ganglia, embryos were harvested and fixed in 4% PFA. Sagittal explants were then made, mounted on glass slides, and imaged to assess sympathetic ganglia formation.

Our data demonstrate that neural crest cells do not sort into normal discrete sympathetic ganglia in the presence of either the ephrinB1-Fc or EphB2-Fc inhibitors (Fig. 2C-E). Strikingly, in ephrinB1-Fc- or EphB2-Fc-injected embryos, EGFP-positive neural crest cells remained dispersed adjacent to the dorsal aorta and failed to condense into discrete ganglia (Fig. 2D,E). By contrast, in control IgG-Fc injected embryos, discrete sympathetic ganglia formed laterally to the rostral half of each somite (Fig. 2C). Analysis of the fluorescence intensities of the EGFP-labeled neural crest cells confirmed the lack of sorting in Eph/ephrin-Fc-injected embryos compared with control IgG-Fc-injected embryos (Fig. 2C-E).

Time-lapse confocal imaging, using sagittal explant cultures, revealed that neural crest cells inhibited by EphB2/ephrinB1 Fc-fusion proteins display intriguing cell migratory behaviors (Fig. 3; see Movie 1 in the supplementary material). Their inability to sort adjacent to the dorsal aorta was not due to an inability to move. To quantify their behavior in relation to their lack of migration away from the inter-ganglionic region, we counted the filopodial extensions of individual neural crest cells at the time when control neural crest cells were sorting into ganglia. In the presence of ephrinB1-Fc, neural crest cells extended and retracted numerous filopodia [ $6 \pm 0.6$  (s.d.);  $P < 0.001$ ] from their entire cell body and further extensions off of these filopodia ( $5.5 \pm 1.0$ ) (Fig. 3F). By contrast, Fc-control injected embryos extended fewer filopodia ( $3.6 \pm 0.79$ ) (Fig. 3F). Taken together, these results show that an increase in filopodia extended from EphB2/ephrinB1-inhibited neural crest cells indicated their ability to sense their environment, but in spite of that, they were unable to respond to signals that would influence them to emigrate from the inter-ganglion region into discrete sympathetic ganglia.

### Fig. 3. Time-lapse analysis of Eph/ephrin Fc-fusion protein injected embryos reveals dynamic neural crest cell behavior.

(A-D) Static images taken from time-lapse movie. Premigratory neural crest cells injected with EGFP. ephrinB1-Fc fusion protein injected in ovo at E3 when neural crest cells were dispersed adjacent to the dorsal aorta. Asterisk indicates location of injection. Sagittal explants cultured at E3.5 and imaged with time-lapse confocal microscopy. At A,  $t=0$ ; at D,  $t=5$  hours. Cells extend and retract numerous filopodia but fail to significantly translocate. Sympathetic ganglia at axial level of fusion protein injection do not sort into ganglia but stay continuous along the dorsal aorta. The dashed circle indicates a region of presumptive sympathetic ganglia. The arrowhead indicates a presumptive inter-ganglionic region. The black arrow indicates time increasing from left to right. (E) An EphB2-Fc injected embryo after 5 hours of incubation. Sympathetic ganglia at level of fusion protein injection (asterisk) do not segregate, but sympathetic ganglia caudal to the injection site segregate normally (brackets), indicating that the inhibitor is only acting at the axial level of the injection. (F) A graph representing the average number of filopodia on neural crest cells in control IgG-Fc injected embryos, and ephrinB1-Fc injected embryos. Control embryos extended  $3.6 \pm 0.79$  (s.d.) filopodia. ephrinB1-Fc injected embryos extended  $6.0 \pm 0.6$  ( $*P < 0.001$ ) filopodia with  $5.5 \pm 1.0$  ( $*P < 0.001$ ) further extensions off primary filopodia (secondary) extended from the cell body. (G) A graph representing the total distance migrated (blue bars) compared to net displacement (purple bars) for individual control and ephrinB1-Fc-inhibited neural crest cells. Scale bars: 40  $\mu\text{m}$  in A-D; 20  $\mu\text{m}$  in E. A, anterior; c, caudal somite; P, posterior; r, rostral somite.



Interestingly, the net displacement in ephrinB1-Fc injected embryos was significantly less than in control embryos (Fig. 3A-D,G). Total distance traveled and net displacement were calculated using time-lapse data sets and cell tracking software, and the directionality calculated (net displacement/total distance traveled). For control injected embryos, neural crest cells had a directionality of  $0.64 \pm 0.133$ , whereas ephrinB1-Fc injected embryos had a directionality of  $0.32 \pm 0.167$  ( $P < 0.001$ ). The total distance traveled and net displacement of 7 neural crest cells in the presence of ephrinB1-Fc and three control neural crest cells are graphed in Fig. 3G. The net displacement of each cell is significantly lower than its overall distance migrated. This measurement indicates that in the presence of ephrinB1-Fc, neural crest cells moved in a less directed manner. Neural crest cells positioned in the inter-ganglionic regions maintained filopodial extensions to neural crest cells in the incipient sympathetic ganglia anterior and posterior to its position (Fig. 3A-D). These neural crest cells persisted in inter-ganglionic regions in the presence of Eph/ephrin blockers with no apparent signs of repulsion at the time when control neural crest cells had sorted into sympathetic ganglia. Intriguingly, cells from the incipient sympathetic ganglion region were even observed entering into and residing within the inter-ganglionic region well after normal segmental sympathetic ganglion formation should have occurred. Interestingly, sympathetic ganglia posterior to the site of EphB2-Fc injection ( $>3$  somite lengths) segregated normally (white brackets; Fig. 3E). Taken together, these data show that sympathetic ganglion sorting is affected only locally, near the area of Fc-fusion protein injections, as posterior sympathetic ganglia sorted normally.

### N-Cadherin is expressed by neural crest cells segregating into discrete sympathetic ganglia

Based on extensive evidence for cadherin regulation as a mechanism that mediates cell aggregation in embryogenesis (Radice et al., 1997; Linask et al., 1998; Bronner-Fraser et al., 1992; Nieto, 2001; Pla et al., 2001), we re-examined the timing of N-cadherin expression in the trunk of E2.5-3.5 chick embryos during sympathetic ganglia formation. In agreement with previous studies, we found that N-cadherin was expressed by neural crest cells as they coalesced to form sympathetic ganglia (Fig. 1C,F) (Bronner-Fraser et al., 1992; Pla et al., 2001). To test N-cadherin function during sympathetic ganglion formation, embryos that had previously been injected with EGFP at HH St. 10 to label premigratory neural crest cells were injected with the blocking N-cadherin antibody, NCD2, in ovo at HH St. 17. The injection and location was carried out in the same manner as Eph/ephrin fusion protein experiments (described above). The NCD2 injected embryos were reincubated for an additional 24 hours. After reincubation, embryos were harvested and fixed, and sagittal explants were made to analyze sympathetic ganglion formation. Analysis of NCD2 injected embryos showed that the shapes of sympathetic ganglia were altered (Fig. 4B). In IgG-control injected embryos, normal sympathetic ganglia formation occurred (Fig. 4A). When we measured the length of sympathetic ganglia in the anteroposterior direction and compared this to the anteroposterior length of the somite at the same axial level in both control and NCD2 injected embryos (Fig. 4C), we noticed dramatic differences. The anteroposterior length of sympathetic ganglia was calculated as the percent of somite length spanned (ratio of sympathetic ganglia length to length of somite at same axial level; Fig. 4E). In IgG-control injected embryos (Fig. 4A), the length of sympathetic ganglia was  $50.0 \pm 2.5\%$  (Fig. 4E, light blue bar) of the length of the somite, corresponding to the length of the rostral somite. In NCD2-blocker injected embryos (Fig. 4B), the length of

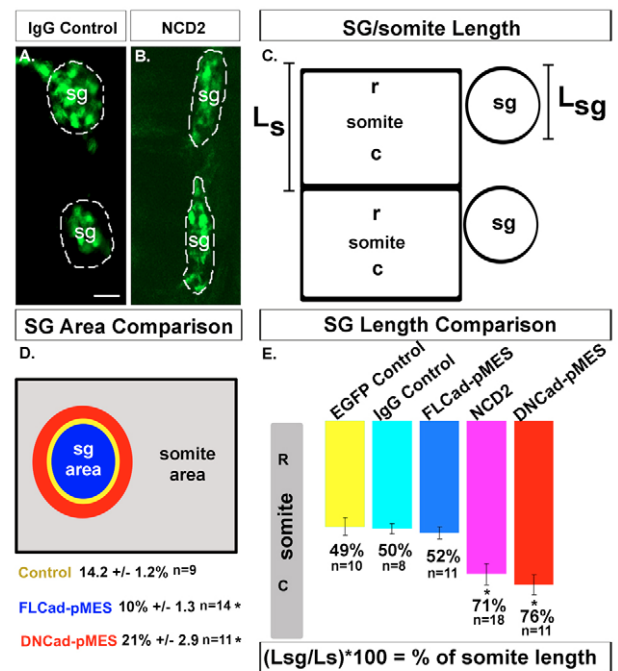


**Fig. 4. Disrupting N-cadherin adhesion in neural crest cells alters sympathetic ganglion formation.** (A, B) EGFP-labeled trunk neural crest cells in anlagen of sympathetic ganglia (dashed circle), E3.5 embryo. (A) IgG control injected embryo with discrete sympathetic ganglion formation. (B) NCD2 in ovo injected embryo analyzed at E3.5. Discrete ganglion formation observed with increase in length (anteroposterior direction), compared to control injected embryos. (C) Schematic showing length comparison of sympathetic ganglia ( $L_{sg}$ ) compared to length of somites ( $L_s$ ) at the same axial level in injected embryos. (D) Area comparison of EGFP control ( $n=9$ ), FL-cadherin ( $n=11$ ;  $*P < 0.001$ ) and DN-cadherin ( $n=14$ ;  $*P < 0.004$ ) electroporated embryos imaged at E3.5 after sympathetic ganglion formation is complete. (E) Length comparison of sympathetic ganglia in control EGFP,  $48.6 \pm 4.1\%$  (s.d.;  $n=10$ ), IgG control inhibitor,  $50.0 \pm 2.5\%$  ( $n=8$ ), FL-cadherin-pMES,  $52.0 \pm 2.9\%$  ( $n=14$ ), NCD2 inhibitor,  $70.5 \pm 4.9\%$  ( $n=18$ ) and DN-cadherin-pMES,  $75.8 \pm 4.6\%$  ( $n=11$ ) electroporated embryos at E3, incubated and imaged at E3.5. Yellow bar, EGFP control electroporated neural crest cells; light blue, IgG control injected blocking antibody into EGFP control labeled embryo; dark blue bar, FL-cadherin electroporated neural crest cells; pink bar, NCD2 blocking antibody injected into EGFP labeled embryos; red bar, DN-cadherin electroporated neural crest cells.  $*P < 0.0001$ . Scale bar:  $40 \mu\text{m}$  in A, B. c, caudal somite; drg, dorsal root ganglia; nt, neural tube; r, rostral somite; sg, sympathetic ganglia.

sympathetic ganglia increased to  $70.5 \pm 4.9\%$  ( $P < 0.0001$ ; Fig. 4E, pink bar) the length of the somite. Thus, sympathetic ganglia were significantly more loosely aggregated in the presence of NCD2 than in control embryos.

As an additional test of the function of N-cadherin in sympathetic ganglion formation, we electroporated dominant-negative cadherin (DN-cadherin) and full-length N-cadherin (FL-cadherin) constructs containing EGFP into premigratory neural crest cells, HH St. 10. The DN-cadherin construct contains only the catenin-binding region of N-cadherin, and has been demonstrated to function as a dominant-negative construct, inhibiting N-cadherin function in vivo (Riehl et al., 1996) (R.B., unpublished). Injecting the cadherin constructs into premigratory neural crest cells will potentially alter their initial migration through the somites, thus affecting their

behavior at the dorsal aorta. This approach was used as a comparison to the function-blocking antibody injections after cells had arrived at the dorsal aorta. After 48 hours of reincubation, electroporated embryos were harvested and fixed. Sagittal explants were then made, mounted on glass slides and imaged to assess sympathetic ganglion formation. We compared the length of sympathetic ganglia to the length of the somite at the same axial level in control (EGFP), DN-cadherin and FL-cadherin electroporated embryos (Fig. 4C,E). In control-electroporated embryos, the length of sympathetic ganglia was  $48.6 \pm 4.1\%$  of the length of the somite (Fig. 4E, yellow bar). In DN-cadherin electroporated embryos, neural crest cells were able to sort into discrete ganglia but the length of sympathetic ganglia increased to  $75.8 \pm 4.6\%$  ( $P \leq 0.0001$ ) of the length of the somite (Fig. 4E, red bar). This  $\sim 60\%$  increase in the length of sympathetic ganglia is nearly the same as in the presence of the NCD2 blocker, indicating that potential defects during their ventral migration does not change the behavior of these cells once at the dorsal aorta. Interestingly, FL-cadherin electroporated embryos had a subtle difference in phenotype versus control embryos. The majority of FL-cadherin-positive cells sorted into ganglia adjacent to the rostral half of each somite, spanning  $52.0 \pm 2.9\%$  of the somite length, similar to control embryos (Fig. 4E, blue bar). However, a subpopulation of cells maintained filopodial connections with other cells across the interganglionic regions between sympathetic ganglia (data not shown). Some filopodia stretched in opposite anteroposterior directions toward different, distinct sympathetic ganglia. This subpopulation of cells did not constitute a dense stream between ganglia but rather filopodial connections and/or single cell bodies interconnecting adjacent ganglia.

In comparison to sympathetic ganglia length and somite size, we measured the two-dimensional area occupied by neural crest cells at presumptive sympathetic ganglia sites in sagittal explants (Fig. 4D). Due to inherent size differences of somites and ganglia at different axial levels, the sympathetic ganglia area was calculated as a percentage of the total area of the somite at the same axial level. Sympathetic ganglia in control electroporated embryos occupied  $14.2 \pm 1.2\%$  of the area of the somite (Fig. 4D, yellow oval). Sympathetic ganglia in DN-cadherin electroporated embryos occupied  $21.0 \pm 2.9$  ( $P < 0.004$ ) of the somite area (Fig. 4D, red oval). This is a  $\sim 50\%$  increase compared with control embryos. FL-cadherin sympathetic ganglia size was  $10.4 \pm 1.3\%$  ( $P < 0.001$ ), a  $\sim 30\%$  decrease compared to control embryos (Fig. 4D, dark blue oval).

To analyze neural crest cell migratory behaviors in response to N-cadherin perturbations, we monitored cell movements using time-lapse confocal imaging. Embryos were electroporated with control EGFP, FL-cadherin or DN-cadherin at HH St. 10, reincubated until HH St. 19-21, and cultured using sagittal explants (Kasemeier et al., 2004). Cell velocities were calculated as cells migrated ventrally through the rostral somite and after neural crest cells had reached ventral locations adjacent to the dorsal aorta, with both calculations being similar in value for each condition (Fig. 5E). Control electroporated neural crest cells migrated at average speeds of  $50 \pm 12.1 \mu\text{m}/\text{hour}$  through the somite and  $62.1 \pm 15.3 \mu\text{m}/\text{hour}$  adjacent to the dorsal aorta ( $n=8$  embryos; Fig. 5E). Interestingly, FL-cadherin electroporated neural crest cells moved  $\sim 75\%$  slower than control electroporated neural crest cells,  $19.3 \pm 5.14 \mu\text{m}/\text{hour}$  through the somite and  $16.2 \pm 2.4 \mu\text{m}/\text{hour}$  adjacent to the dorsal aorta ( $n=7$  embryos;  $P < 0.01$ ; Fig. 5E). DN-cadherin neural crest cells also moved more slowly (53%) than control neural crest cells, at  $24.7 \pm 4.6 \mu\text{m}/\text{hour}$  through the somite

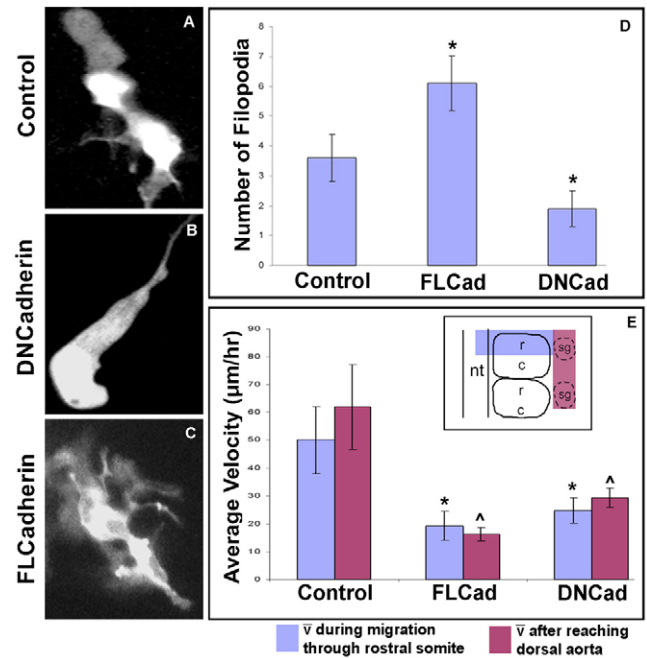


**Fig. 5. Cell shape and velocity comparisons in neural crest cells transfected with EGFP, DN-cadherin or FL-cadherin.** Cells imaged at E3-3.5 during sympathetic ganglion formation adjacent to the dorsal aorta. (A) Control EGFP-expressing neural crest cells. (B) FL-cadherin-expressing neural crest cell. (C) DN-cadherin-expressing neural crest cells. (D) Graph of number of filopodia on cells expressing EGFP control,  $3.6 \pm 0.79$  (s.d.), FL-cadherin,  $6.1 \pm 0.91$  and DN-cadherin,  $1.9 \pm 0.6$ . (E) Graph showing average cell velocities during ventral migration and after reaching dorsal aorta. The schematic shows the region within the embryo that cells were migrating through when the velocity was measured. Ventral migration through the rostral somite for EGFP control,  $50 \pm 12.1 \mu\text{m}/\text{hour}$ , FL-cadherin,  $19.3 \pm 5.14 \mu\text{m}/\text{hour}$ , and DN-cadherin,  $24.7 \pm 4.63 \mu\text{m}/\text{hour}$ . Cell velocities after reaching dorsal aorta, EGFP control  $62.1 \pm 15.3 \mu\text{m}/\text{hour}$ , FL-cadherin,  $16.2 \pm 2.4 \mu\text{m}/\text{hour}$ , and DN-cadherin,  $29.2 \pm 3.5 \mu\text{m}/\text{hour}$ . Asterisk and caret (D,E) indicate significance,  $P < 0.01$ ,  $P < 0.001$ , respectively. Scale bars:  $10 \mu\text{m}$  in A-C;  $20 \mu\text{m}$  in D, E. c, caudal somite; r, rostral somite.

and  $29.2 \pm 3.5 \mu\text{m}/\text{hour}$  adjacent to the dorsal aorta ( $n=8$  embryos;  $P < 0.001$ ; Fig. 5E). The introduction of different N-cadherin constructs also altered cell morphologies; there were significant differences in the numbers and disposition of filopodia (Fig. 5A-C). Measurements of filopodia may indicate the ability of the cells to adhere and coalesce into compact ganglia. Neural crest cells overexpressing FL-cadherin possessed numerous filopodia,  $6.1 \pm 0.91$  ( $P < 0.001$ ), that extended and contacted cells in all directions (Fig. 5C,D). Control cells tended to have  $\sim 60\%$  fewer filopodia ( $3.6 \pm 0.79$ ), but the filopodia were longer and thicker than those extended by FL-cadherin cells (Fig. 5A,C-D). By contrast, DN-cadherin cells displayed  $\sim 50\%$  fewer filopodia ( $1.9 \pm 0.6$ ;  $P < 0.001$ ) than control cells and were mostly extended in a bipolar direction from the cell body (Fig. 5B,D). The number and thickness of filopodia correlates with ability of cells to potentially adhere to one another through cadherins. DN-cadherin expressing cells possessed fewer filopodia, correlating with the larger ganglion size seen above. Increasing the number of longer and thicker filopodia using FL-cadherin did not correlate with smaller ganglia, which indicates there is a limit at which more filopodia do not affect ganglion size.

## DISCUSSION

The segregation of trunk neural crest cells into discrete migratory streams that lead from the neural tube to the dorsal aorta have long been thought to be the basis for the metameric organization of sympathetic ganglia (Bronner-Fraser, 1986; Lallier and Bronner-Fraser, 1988; Oakley and Tosney, 1993; Keynes and Stern, 1988). Yet, our recent time-lapse analyses revealed that neural crest cells arrive at the dorsal aorta, then spread out along the anteroposterior directions and intermingle with neighboring neural crest cell migratory streams before undergoing a second resorting process (Kasemeier-Kulesa et al., 2005). Elegant work published by Yip (Yip, 1986) had previously demonstrated that neural crest cells that contribute to a given sympathetic ganglion can arise from up to two segments rostrally and three segments caudally to that sympathetic ganglion. However, with his methods he was unable to identify where the cell mixing was occurring, i.e. in the neural tube, en route or at the target site. Although our work did not preclude cell mixing at earlier time points, it clearly demonstrated cell mixing at the target site. We hypothesized that a separate set of local cues at the sympathetic ganglia target locations sculpt neural crest cells into discrete structures. Our goal here was to identify and shed light on the molecular mechanisms that mediate the formation of discrete sympathetic ganglia. After careful gene expression analysis correlated neural crest cell positions to potential molecular candidates, we used blocking agents, expression vectors and intravital confocal 3D time-lapse imaging to measure changes in neural crest cell migratory behaviors and sympathetic ganglia size. Using our novel sagittal explant culture technique and application of blockers locally, we were able to wait until neural crest cells had completed their initial ventral migration, such that we would perturb only the neural crest cells at the dorsal aorta as they were redistributing and sorting into discrete ganglia.

### Distinct gene expression patterns correlate with cell movements during sympathetic ganglia formation

Our goal in this study was to identify and understand the molecular mechanisms that mediate the secondary sorting (re-sorting) of trunk neural crest cells into discrete sympathetic ganglia. Our results demonstrate two mechanisms that sculpt the formation of sympathetic ganglia (Fig. 6). The first mechanism involves the emergence of ephrinB1 ligand expression in the inter-ganglionic region that drives cells away and restricts cells from coalescing in the inter-ganglionic region. Eph receptors on neural crest cells and the emergence of ephrin ligands expressed in domains adjacent to the ventral edge of the caudal somite inhibit neural crest cells from remaining in the region ventral to the caudal somite. This forces neural crest cells to accumulate in regions immediately adjacent to the rostral somite, which is devoid of ephrinB1. Secondly, cells are influenced within a regional domain via homophilic adhesion molecules. As neural crest cells accumulate in closer proximity to one another (migrating away from ephrinB1-positive regions), N-cadherin expressed on these cells signals them to adhere to one another. These two distinct cellular behaviors mediated by inhibitory and adhesive mechanisms ultimately work together to sculpt the emergence of discrete sympathetic ganglia (Fig. 6).

Our results identify the need for both adhesive and repulsive mechanisms in ganglion formation, suggesting a tight spatiotemporal coordination between the local tissue microenvironment and neural crest cell movements. EphrinB1 ligand expression in the caudal somite (HH St. 17) extends in to the inter-ganglionic region (HH St. 20) over the period when EphB2-

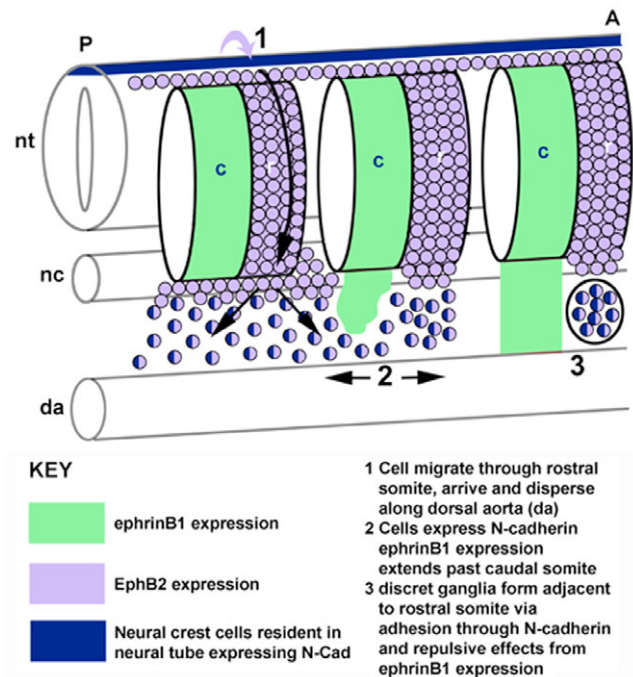


**Fig. 6. Model of events needed for proper sympathetic ganglion formation.** Schematic model showing important events in a spatiotemporal pattern for discrete sympathetic ganglion formation adjacent to the ventral edge of a rostral somite. **1.** Neural crest cells migrate from the neural tube through the rostral somites. **2.** Neural crest cells disperse adjacent to the dorsal aorta. ephrinB1 expression is established in inter-ganglionic regions between developing ganglia. **3.** N-cadherin adhesion and inhibitory ephrinB1 expression induce formation of discrete ganglia. A, anterior; c, caudal somite; da, dorsal aorta; nc, notochord; nt, neural tube; P, posterior; r, rostral somite.

expressing neural crest cells retreat from inter-ganglionic regions (Fig. 1). During this developmental window, neural crest cells express N-cadherin (Fig. 1). Eph receptors and their ephrin ligands are key players controlling the position of tissue boundaries during multiple events in embryonic development through their ability to mediate cell sorting (Davy et al., 2004; Sela-Donenfeld and Wilkinson, 2005). Xu et al. (Xu et al., 1999) showed that activation of Eph receptors or ephrins can also drive cell sorting in rhombomeres of the zebrafish. In addition to restricting trunk neural crest cell migration to the rostral somite halves (Wang and Anderson, 1997; Krull et al., 1997), Eph/ephrins play key roles in repulsive guidance of axonal growth cones (Poliakov et al., 2004). Our results agree with Xu et al. (Xu et al., 1999), that adhesive systems can be coupled with Eph/ephrins to orchestrate cellular organization of tissues.

### Sympathetic ganglia form from an interplay of cell sorting and cell adhesion

What role do EphB/ephrinB interactions play during formation of sympathetic ganglia? We used ephrinB1-Fc to block and interfere with any receptors that would normally bind to ephrinB1, and alternatively used EphB2-Fc to block and interfere with any ligands that normally bind to EphB2 (Fig. 2). Obtaining similar results with both fusion proteins suggests that these two molecules are indeed interacting and operative during the second sorting process of sympathetic ganglia into discrete ganglia. Although we cannot rule out that EphB2 and ephrinB1 could also interact with other ephrin

ligands or Eph receptors, our expression studies did not reveal appropriate spatiotemporal expression patterns for other family members we examined.

Recently, Eph/ephrins have been shown to signal both in forward (through the receptor) and reverse (through the ligand) direction signaling (Davy et al., 2004). However, as demonstrated in our expression analysis and those of Krull et al. (Krull et al., 1997) and Santiago and Erickson (Santiago and Erickson, 2002), ephrinBs are not expressed on neural crest cells; hence reverse signaling is not a potential mechanism in our system. Thus our work identifies a novel function for ephrinB1 in the life of a trunk neural crest cell that will give rise to sympathetic ganglia.

### N-Cadherin controls ganglion size

What functions are adhesion molecules mediating during sympathetic ganglion formation? Blocking N-cadherin when neural crest cells were dispersed along the dorsal aorta interfered with the normal compaction of neural crest cells into tightly coalesced sympathetic ganglia (Fig. 4). Interestingly, overexpression of FL-cadherin resulted in no significant difference in ganglion length but a decrease in area. The increased intercellular adhesion induced by ectopic expression of N-cadherin apparently induces compaction of the ganglion without altering the length of cells along the anteroposterior axis. This is possibly due to the observation that some inter-ganglionic connections are still maintained, evidenced by persisting filopodial connections between ganglia. Additionally, the cells may be as tightly coalesced in the anteroposterior direction as they can be, so a difference is only observed when the overall area is calculated. Neural crest cells migrated normally, away from the inter-ganglionic region where inhibitory interactions between Eph/ephrins occur; however, many neural crest cells maintained filopodial extensions within the inter-ganglionic region, and as a result the sympathetic ganglia that formed were less compact (Fig. 5). We hypothesize that this is due to a decrease in local cell adhesion. Time-lapse analyses of neural crest cells in FL-cadherin- and DN-cadherin-electroporated embryos revealed striking differences in average cell velocities (Fig. 5). FL-cadherin neural crest cells presumably express more N-cadherin on their surface, increasing the potential to form homophilic adhesions with other cells expressing N-cadherin. Thus, they undergo an increase in cell-to-cell contacts, and hence move more slowly. We predict that with fewer functional cadherin molecules expressed on the surface of a cell, these neural crest cells would move faster than control cells, but in fact they do not. Pla et al. (Pla et al., 2001) showed that dissociated, isolated neural crest cells in culture did not migrate, suggesting that cells may need a 'baseline' of contacts with one another to migrate, and below this threshold they do not move due to lack of communication with their neighbors. Thus, both excess and limited N-cadherin-mediated cell adhesion perturbs the behavior of neural crest cells and disrupts normal formation of sympathetic ganglia.

Taken together, our data indicate that cell adhesion and inhibitory mechanisms work together to sort neural crest cells into discrete sympathetic ganglia. N-Cadherin has also been shown to influence cellular condensation in cartilage formation (Tuan, 2003). As N-cadherin is expressed in multiple tissues at several time points in the developing embryo, it is not surprising that it can act during two stages of neural crest cell development: First, in neural tube formation and later to promote aggregation of sympathetic ganglia. Studies have also shown that differential expression of cell adhesion molecules within mixed cell populations can lead to cell sorting (Friedlander et al., 1989; Nose et al., 1988). In our system, we are presumably dealing with one cell type during the sorting of neural

crest cells into discrete sympathetic ganglia, and our data do not preclude a role for other adhesion molecules in the aggregation of neural crest cells as the cells form sympathetic ganglia. There is currently no evidence to support a model for a single cell adhesion molecule capable of forming a patterned structure, such as the metamer pattern of sympathetic ganglia.

In summary, our data indicate that both adhesive and repulsive mechanisms are necessary for the sculpting of discrete sympathetic ganglia. Using our novel sagittal explant culture technique and application of blockers locally, we were able to wait until neural crest cells had completed their initial ventral migration, such that we would perturb only the neural crest cells at the dorsal aorta as they were redistributing and sorting into discrete ganglia. Together, our data indicate that medial-to-lateral cues in the somite ensure that sympathetic ganglion precursor cells arrive adjacent to the dorsal aorta. Neural crest cells then respond to anteroposterior cues that refine the pattern of metamer ganglia. If cells were strictly responding to Eph/ephrin repulsive instructions, there would be no cue driving neural crest cells to form compact ganglia. If the cells were solely responding to the N-cadherin-mediated adhesion there would be no instructions for them to sort into a metamer pattern throughout the axis of the embryos. Thus, we suggest that neural crest cells integrate repulsive (Eph-ephrin) cues in inter-ganglionic regions and attractive (N-cadherin) cues to sort into discrete sympathetic ganglia. Future investigations of primary sympathetic ganglion formation will have the challenge of elucidating the simultaneous signaling events of multiple molecules.

We thank Dr Cathy Krull (University of Michigan) for the pMES vector, and Danny Stark (Stowers Institute) for imaging assistance. This work was supported by the Stowers Institute for Medical Research and from grant support to F.L. from the National Institutes of Health, NS35714, J.C.K.K. from NIH-NCRR, P20-RR-16455 and P. Kopriva Foundation (M.S.U.).

### Supplementary material

Supplementary material for this article is available at <http://dev.biologists.org/cgi/content/full/133/24/4839/DC1>

### References

- Bronner-Fraser, M. (1986). Analysis of the early stages of trunk neural crest migration in avian embryos using monoclonal antibody HNK-1. *Dev. Biol.* **115**, 44-55.
- Bronner-Fraser, M., Wolf, J. J. and Murray, B. A. (1992). Effects of antibodies against N-cadherin and N-CAM on the cranial neural crest and neural tube. *Dev. Biol.* **153**, 291-301.
- Davy, A., Aubin, J. and Soriano, P. (2004). Ephrin-B1 forward and reverse signaling are required during mouse development. *Genes Dev.* **18**, 572-583.
- Friedlander, D. R., Mege, R.-M., Cunningham, B. A. and Edelman, G. M. (1989). Cell sorting-out is modulated by both the specificity and amount of different cell adhesion molecules (CAMs) expressed on cell surfaces. *Proc. Natl. Acad. Sci. USA* **86**, 7043-7047.
- Garcia-Castro, M. I., Vielmetter, E. and Bronner-Fraser, M. (2000). N-Cadherin, a cell adhesion molecule involved in establishment of embryonic left-right asymmetry. *Science* **288**, 1047-1051.
- Hamburger, V. and Hamilton, H. L. (1951). A series of normal stages in the development of the chick embryo. *J. Morphol.* **88**, 49-92.
- Holash, J. A., Soans, C., Chong, L. D., Shao, H., Dixit, V. M. and Pasquale, E. B. (1995). Reciprocal expression of the Eph receptor Cdk5 and its ligand(s) in the early retina. *Dev. Biol.* **182**, 256-269.
- Kasemeier, J. C., Lefcort, F., Fraser, S. E. and Kulesa, P. M. (2004). A novel sagittal slice explant technique for time-lapse imaging of the formation of the chick peripheral nervous system. In *Imaging in Neuroscience and Development* (ed. R. Yuste and A. Konnerth). Cold Spring Harbor, NY: Cold Spring Harbor Laboratory Press.
- Kasemeier-Kulesa, J. C., Kulesa, P. M. and Lefcort, F. (2005). Imaging neural crest cell dynamics during formation of dorsal root ganglia and sympathetic ganglia. *Development* **132**, 235-245.
- Keynes, R. J. and Stern, C. D. (1988). Mechanisms of vertebrate segmentation. *Development* **103**, 413-429.
- Koblar, S. A., Krull, C. E., Pasquale, E. B., McLennan, R., Peale, F. D., Cerretti, D. P. and Bothwell, M. (2000). Spinal motor axons and neural crest cells use



- different molecular guides for segmental migration through the rostral half-somite. *J. Neurobiol.* **42**, 437-447.
- Kontges, G. and Lumsden, A.** (1996). Rhombencephalic neural crest segmentation is preserved throughout craniofacial ontogeny. *Development* **122**, 3229-3242.
- Krull, C. E. and Kulesa, P. M.** (1998). Embryonic explant and slice preparations for studies of cell migration and axon guidance. In *Cellular and Molecular Procedures in Developmental Biology* (ed. F. dePablo, A. Ferrus and C. D. Stern), pp. 145-159. San Diego, CA: Academic Press.
- Krull, C. E., Collazo, A., Fraser, S. E. and Bronner-Fraser, M.** (1995). Segmental migration of trunk neural crest: time-lapse analysis reveals a role for PNA-binding molecules. *Development* **121**, 3733-3743.
- Krull, C. E., Lansford, R., Gale, N. W., Collazo, A., Marcelle, C., Yancopoulos, G. D., Fraser, S. E. and Bronner-Fraser, M.** (1997). Interactions of Eph-related receptors and ligands confer rostrocaudal pattern to trunk neural crest migration. *Curr. Biol.* **7**, 571-580.
- Kulesa, P. M. and Fraser, S. E.** (2000). In ovo time-lapse analysis of chick hindbrain neural crest cell migration shows cell interactions during migration to the brachial arches. *Development* **127**, 1161-1172.
- Lallier, T. E. and Bronner-Fraser, M.** (1988). A spatial and temporal analysis of dorsal root ganglia and sympathetic ganglia formation in the avian embryo. *Dev. Biol.* **127**, 99-112.
- LeDouarin, N. M. and Kalcheim, C.** (1999). *The Neural Crest*. Cambridge, UK: Cambridge University Press.
- Linask, K. K., Ludwig, C., Han, M.-D., Liu, X., Radice, G. L. and Knudsen, K. A.** (1998). N-Cadherin/catenin-mediated morphoregulation of somite formation. *Dev. Biol.* **202**, 85-102.
- Loring, J. F. and Erickson, C. A.** (1987). Neural crest cell migratory pathways in the trunk of the chick embryo. *Dev. Biol.* **121**, 220-236.
- Newgreen, D. F., Scheel, M. and Kastner, V.** (1986). Morphogenesis of sclerotome and neural crest in avian embryos. In vivo and in vitro studies on the role of notochordal extracellular material. *Cell Tissue Res.* **244**, 229-313.
- Nieto, M. A.** (2001). The early steps of neural crest development. *Mech. Dev.* **105**, 27-35.
- Nose, A., Nagafuchi, A. and Takeichi, M.** (1988). Expressed recombinant Cadherins mediate cell sorting in model systems. *Cell* **54**, 993-1001.
- Oakley, R. A. and Tosney, K. W.** (1993). Contact-mediated mechanisms of motor axon segmentation. *J. Neurosci.* **13**, 3776-3792.
- Pla, P., Moore, R., Morali, O. G., Grille, S., Martinozzi, S., Delmas, V. and Larue, L.** (2001). Cadherins in neural crest cell development and transformation. *J. Cell Physiol.* **189**, 121-132.
- Poliakov, A., Cotrina, M. and Wilkinson, D. G.** (2004). Diverse roles of eph receptors and ephrins in the regulation of cell migration and tissue assembly. *Dev. Cell* **7**, 465-480.
- Radice, G. L., Rayburn, H., Matsunami, H., Knudsen, K. A., Takeichi, M. and Hynes, R. O.** (1997). Developmental defects in mouse embryos lacking N-Cadherin. *Dev. Biol.* **181**, 64-78.
- Rickmann, M., Fawcett, J. W. and Keynes, R. J.** (1985). The migration of neural crest cells and the growth of motor axons through the rostral half of the chick somite. *J. Embryol. Exp. Morphol.* **90**, 437-455.
- Riehl, R., Johnson, K., Bradley, R., Grunwald, G. B., Cornel, E., Lilienbaum, A. and Holt, C. E.** (1996). Cadherin function is required for axon outgrowth from retinal ganglion cells in vivo. *Neuron* **17**, 837-848.
- Rifkin, J. T., Todd, V. J., Anderson, L. W. and Lefcort, F.** (2000). Dynamic expression of neurotrophin receptors during sensory neuron genesis and differentiation. *Dev. Biol.* **227**, 465-480.
- Santiago, A. and Erickson, C. A.** (2002). Ephrin-B ligands play a dual role in the control of neural crest cell migration. *Development* **129**, 3621-3632.
- Schilling, T. F. and Kimmel, C. B.** (1994). Segment and cell type lineage restrictions during pharyngeal arch development in the zebrafish embryo. *Development* **120**, 483-494.
- Sela-Donenfeld, D. and Wilkinson, D. G.** (2005). Eph receptors: two ways to sharpen boundaries. *Curr. Biol.* **15**, R210-R212.
- Tosney, K. W. and Oakley, R. A.** (1990). The perinotochordal mesenchyme acts as a barrier to axon advance in the chick embryo: implications for a general mechanism of axonal guidance. *Exp. Neurol.* **109**, 75-89.
- Trainor, P. and Krumlauf, R.** (2002). Development. Riding the crest of the Wnt signaling wave. *Science* **297**, 781-783.
- Tuan, R. S.** (2003). Cellular signaling in developmental chondrogenesis: N-cadherin, Wnts, and BMP-2. *J. Bone Jt Surg. Am.* **85**, 134-141.
- Wang, H. U. and Anderson, D. J.** (1997). Eph family transmembrane ligands can mediate repulsive guidance of trunk neural crest migration and motor axon outgrowth. *Neuron* **18**, 383-396.
- Xu, Q., Mellitzer, G., Robinson, V. and Wilkinson, D. J.** (1999). In vivo cell sorting in complementary segmental domains mediated by Eph receptors and ephrins. *Nature* **339**, 267-271.
- Yip, J. W.** (1986). Migratory patterns of sympathetic ganglioblasts and other neural crest derivatives in chick embryos. *J. Neurosci.* **6**, 3465-3474.